Bitopic Phenylene-Linked Bis(pyrazolyl)methane Ligands: Preparation and Supramolecular Structures of Hetero- and Homobimetallic Complexes Incorporating Organoplatinum(II) and Tricarbonylrhenium(I) Centers

Daniel L. Reger,* Russell P. Watson, Mark D. Smith, and Perry J. Pellechia

Department of Chemistry and Biochemistry, University of South Carolina, Columbia, South Carolina 29208

Received November 16, 2004

The new fixed-geometry, phenylene-linked bis(pyrazolyl)methane ligands α,α,α′,α′-tetra(1-pyrazolyl)-*m*-xylene (*m*-$[CH(pz)_2]_2C_6H_4$, $\mathbf{L}_m$), α,α,α′,α′-tetra(1-pyrazolyl)-*p*-xylene (*p*-$[CH(pz)_2]_2C_6H_4$, $\mathbf{L}_p$), and α,α,α′,α′-tetrakis(4-benzylpyrazol-1-yl)-*p*-xylene (*p*-$[CH(^{4Bn}pz)_2]_2C_6H_4$, $^{4Bn}\mathbf{L}_p$) have been synthesized in order to prepare hetero- and homobimetallic complexes incorporating tricarbonylrhenium(I) and bis(*p*-tolyl)platinum(II) fragments. Coordination of one rhenium center to $\mathbf{L}_m$ was achieved to yield the monometallic rhenium complex {*m*-$[CH(pz)_2]_2C_6H_4$}$Re(CO)_3Br$, which then incorporated a second metal center to give the heterobimetallic complex {*μ*-*m*-$[CH(pz)_2]_2C_6H_4$}$[Re(CO)_3Br][Pt(p\text{-tolyl})_2]$. The homobimetallic rhenium complexes of each ligand, {*μ*-*m*-$[CH(pz)_2]_2C_6H_4$}$[Re(CO)_3Br]_2$, {*μ*-*p*-$[CH(pz)_2]_2C_6H_4$}$[Re(CO)_3Br]_2$, and {*μ*-*p*-$[CH(^{4Bn}pz)_2]_2C_6H_4$}$[Re(CO)_3Br]_2$, were also prepared. The crystalline structure of each complex shows extensive noncovalent interactions, including weak hydrogen bonds and $\pi\cdots\pi$ and $CH\cdots\pi$ interactions, that organize the molecules into complex supramolecular structures.

Introduction

Homo- and heteromultimetallic complexes have been intensely studied in search of reactivity not observed for their monometallic counterparts.[1] For example, some catalytic processes employing bi- or multimetallic complexes have been found to proceed with efficiencies greater than those catalyzed by the corresponding monometallic species.[2,3] Heterobimetallic catalysts also offer the possibility of tandem catalytic processes as in recent examples of olefin polymerization in which one site produces a specific type of polymer that is immediately incorporated into another type of polymer produced by the other proximate metal center.[4] One method to prepare such complexes is the use of bitopic ligands, but the syntheses of heterometallic complexes of such ligands are more challenging than those of homometallic complexes because of the need to initially prepare selectively a monometallic intermediate.[5] Other paths to heterometallic complexes do exist, such as the coupling of two monometallic complexes or the coupling of a monometallic complex with a ligand followed by introduction of the second metal,[6] but the preparation from the bitopic ligand is often difficult if not unfeasible. We are actively developing synthetic routes to homo- and heterometallic complexes using multitopic ligands based on linking multiple poly(pyrazolyl)methane donor units in a single molecule. We have prepared multitopic ligands in which poly(pyrazolyl)methane fragments are linked by flexible,[7] semirigid,[8] and rigid[9] organic spacers. For example, we recently reported the structures and supramolecular organizations of cyclic silver(I) bimetallic complexes using the flexible alkylidene-linked

* To whom correspondence should be addressed. E-mail: reger@mail.chem.sc.edu.

(1) (a) Ceccon, A.; Santi, S.; Orian, L.; Bisello, A. *Coord. Chem. Rev.* **2004**, *248*, 683. (b) Fulton, J. R.; Hanna, T. A.; Bergman, R. G. *Organometallics* **2000**, *19*, 602. (c) Fukuoka, A.; Fukagawa, S.; Hirano, M.; Koga, N.; Komiya, S. *Organometallics* **2001**, *20*, 2065. (d) Fabre, S.; Findeis, B.; Trösch, D. J. M.; Gade, L. H.; Scowen, I. J.; McPartlin, M. *Chem. Commun.* **1999**, 577. (e) Schubart, M.; Mitchell, G.; Gade, L. H.; Kottke, T.; Scowen, I. J.; McPartlin, M. *Chem. Commun.* **1999**, 233. (f) Scheider, A.; Gade, L. H.; Breuning, M.; Bringman, G.; Scowen, I. J.; McPartlin, M. *Organometallics* **1998**, *17*, 1642. (g) *Catalysis by Di- and Polynuclear Metal Cluster Complexes*; Adams, R. D., Cotton, F. A., Eds.; Wiley-VCH: New York, 1998, and references therein.

(2) (a) Trost, B. M.; Mino, T. *J. Am. Chem. Soc.* **2003**, *125*, 2410. (b) Jacobsen, E. N. *Acc. Chem. Res.* **2000**, *33*, 421. (c) Molenveld, P.; Engbersen, J. F. J.; Reinhoudt, D. N. *Chem. Soc. Rev.* **2000**, *29*, 75. (d) Sawamura, M.; Sudoh, M.; Ito, Y. *J. Am. Chem. Soc.* **1996**, *118*, 3309. (d) Broussard, M. E.; Juma, B.; Train, S. G.; Peng, W.-J.; Laneman, S. A.; Stanley, G. G. *Science* **1993**, *260*, 1784.

(3) (a) Guo, N.; Li, L.; Marks, T. J. *J. Am. Chem. Soc.* **2004**, *126*, 6542. (b) Li, H.; Li, L.; Marks, T. J.; Liable-Sands, L.; Rheingold, A. L. *J. Am. Chem. Soc.* **2003**, *125*, 10788. (c) Li, L.; Metz, M. V.; Li, H.; Chen, M.-C.; Marks, T. J.; Liable-Sands, L.; Rheingold, A. L. *J. Am. Chem. Soc.* **2002**, *124*, 12725.

(4) (a) Wang, J.; Li, H.; Guo, N.; Li, L.; Stern, C. L.; Marks, T. J. *Organometallics* **2004**, *23*, 5112. (b) Abramo, G. P.; Li, L.; Marks, T. J. *J. Am. Chem. Soc.* **2002**, *124*, 13966.

(5) (a) Balzani, V.; Juris, A.; Venturi, M.; Campagna, S.; Serroni, S. *Chem. Rev.* **1996**, *96*, 759. (b) Chong, S. H.-F.; Lam, S. C.-F.; Yam, V. W.-W.; Zhu, N.; Cheung, K.-K.; Fathallah, S.; Costuas, K.; Halet, J.-F. *Organometallics* **2004**, *23*, 4924. (c) Masllorens, J.; Roglans, A.; Moreno-Mañas, M.; Parella, T. *Organometallics* **2004**, *23*, 2533.

(6) (a) Harriman, A.; Hissler, M.; Khatyr, A.; Ziessel, R. *Eur. J. Inorg. Chem.* **2003**, 955. (b) Börje, A.; Köthe, O.; Juris, A. *J. Chem. Soc., Dalton Trans.* **2002**, 843.

(7) (a) Reger, D. L.; Watson, R. P.; Gardinier, J. R.; Smith, M. D. *Inorg. Chem.* **2004**, *43*, 6609. (b) Reger, D. L.; Gardinier, J. R.; Semeniuc, R. F.; Smith, M. D. *J. Chem. Soc., Dalton Trans.* **2003**, 1712. (c) Reger, D. L.; Gardinier, J. R.; Grattan, T. C.; Smith, M. R.; Smith, M. D. *New J. Chem.* **2003**, *27*, 1670.

(8) (a) Reger, D. L.; Brown, K. J.; Gardinier, J. R.; Smith, M. D. *Organometallics* **2003**, *22*, 4973.

(9) Reger, D. L.; Gardinier, J. R.; Smith, M. D. *Polyhedron* **2004**, *23*, 291.

10.1021/om049112f CCC: $30.25
Publication on Web 02/22/2005

bis(pyrazolyl)methane ligands $CH(pz)_2(CH_2)_nCH(pz)_2$ (pz = 1-pyrazolyl; $n = 1, 2, 3$).[7] We have also extensively developed the chemistry of the semirigid multitopic tris(pyrazolyl)methane ligands $C_6H_{6-n}[CH_2OCH_2C(pz)_3]_n$, where $n = 2$, 3 4, and 6.[10] Our studies thus far have revealed that in the solid state poly(pyrazolyl)methane compounds often support important noncovalent interactions such as weak hydrogen bonds, $\pi\cdots\pi$ stacking, and C−H$\cdots\pi$ interactions.[11] In particular we have identified an important structural feature in which two pairs of adjacent pyrazolyl rings are noncovalently associated through cooperative CH$\cdots\pi$ and $\pi\cdots\pi$ interactions. We have found that these interactions are common not only in our compounds but in a large number of known poly(pyrazolyl)borate and -methane compounds, and we have termed this supramolecular motif the "quadruple pyrazolyl embrace".[7b] We are interested in contrasting the molecular and supramolecular structures of complexes of rigid ligands with the more flexible counterparts studied earlier. Our previous efforts in preparing complexes of rigid ligands containing tridentate tris(pyrazolyl)methane units, however, have been limited by solubility problems.[9]

Herein we describe the synthesis of three rigidly linked *bitopic* bis(pyrazolyl)methane ligands, *m*-$C_6H_4[CH(pz)_2]_2$ (**L*m***), *p*-$C_6H_4[CH(pz)_2]_2$ (**L*p***), and *p*-$C_6H_4[CH(^{4Bn}pz)_2]_2$ (**^{4Bn}L*p***; ^{4Bn}pz = 4-benzyl-1-pyrazolyl), and the use of these ligands to prepare the homobimetallic complexes {μ-*m*-$[CH(pz)_2]_2C_6H_4$}$[Re(CO)_3Br]_2$ (**3**), {μ-*p*-$[CH(pz)_2]_2C_6H_4$}$[Re(CO)_3Br]_2$ (**4**), and {μ-*p*-$[CH(^{4Bn}pz)_2]_2C_6H_4$}$[Re(CO)_3Br]_2$ (**5**). We also report the first heterobimetallic complex of a linked bis(pyrazolyl)methane ligand, {μ-*m*-$[CH(pz)_2]_2C_6H_4$}$[Re(CO)_3Br][Pt(p\text{-tolyl})_2]$ (**2**), prepared from monometallic {*m*-$[CH(pz)_2]_2C_6H_4$}$Re(CO)_3Br$ (**1**). In the solid state, each complex shows extensive noncovalent interactions that organize the molecules into complex supramolecular structures.

Experimental Section

General Considerations. Air-sensitive materials were handled under a nitrogen atmosphere using standard Schlenk techniques or in a Vacuum Atmospheres HE-493 drybox. All solvents were dried and distilled by conventional methods prior to use. $Re(CO)_5Br$,[12] $[Pt(SEt_2)(p\text{-tolyl})_2]_2$,[13] 1,1′-carbonyldipyrazole,[14] and 4-benzylpyrazole[7c] were prepared following reported procedures. All other chemicals were purchased from Aldrich or Fisher Scientific. Pyrazole was purified by sublimation prior to use. Thionyl chloride was distilled prior to use. All other purchased chemicals were used as received. Reported melting points are uncorrected. IR spectra were obtained on a Nicolet 5DXBO FTIR spectrometer. ^{1}H and ^{13}C NMR spectra were recorded on a Mercury/VX 300, Mercury/VX 400, or INOVA 500 spectrometer. All chemical shifts are in ppm and are secondary referenced using the solvent signals. Mass spectrometric measurements were obtained on a MicroMass QTOF spectrometer or on a VG 70S instrument. Elemental analyses were performed on vacuum-dried samples by Robertson Microlit Laboratories (Madison, NJ).

α,α,α′,α′-Tetra(1-pyrazolyl)-*m*-xylene, *m*-$[CH(pz)_2]_2C_6H_4$ (L*m*). CO(pz)$_2$ Method. Isophthalaldehyde (1.57 g, 11.7 mmol), 1,1′-carbonyldipyrazole (4.817 g, 29.7 mmol), and anhydrous cobalt chloride (0.32 g, 2.5 mmol) were dissolved in 100 mL of anhydrous THF and heated at reflux for 24 h. After cooling to room temperature, 50 mL of distilled water was added, and the solution was stirred for 30 min and extracted with CH_2Cl_2 (3 × 50 mL). The combined organic extracts were washed with concentrated NaCl solution and dried over $MgSO_4$. The solution was then concentrated and chromatographed (silica gel, Et_2O) to afford 2.55 g (59% yield) of a white solid. Mp: 129−130 °C. Anal. Calcd for $C_{20}H_{18}N_8$: C, 64.86; H, 4.90; N, 30.25. Found: C, 64.53; H, 4.95; N, 30.41. IR (KBr, cm^{-1}): 3138, 3113, 3101, 2999, 2942, 2897, 2823, 2692, 2656, 2623, 1736, 1601, 1516. ^{1}H NMR (300 MHz, acetone-d_6): δ 7.93 (s, 2 H, C*H*(pz)$_2$), 7.76 (dd, J = 2.4, 0.6 Hz, 4 H, 5-H pz), 7.53 (dd, J = 2.0, 0.6 Hz, 4 H, 3-H pz), 7.40 (t, J = 8.0 Hz, 1 H, 5-H C_6H_4), 7.08 (d, J = 7.8 Hz, 2 H, 4,6-H C_6H_4), 6.80 (s, 1 H, 2-H C_6H_4), 6.31 (dd, J = 2.6, 2.0 Hz, 4 H, 4-H pz). ^{13}C NMR (75.5 MHz, acetone-d_6): δ 140.3, 138.2, 130.2, 129.0, 127.8, 126.1, 106.4, 77.1. HRMS: calcd for $C_{20}H_{18}N_8$, 370.1654; found, 370.1662. Direct Probe MS *m/z* (rel int %) [assgn]: 370 (5) $[M]^+$, 302 (100) $[M - Hpz]^+$, 235 (95) $[M - Hpz - pz]^+$.

SO(pz)$_2$ Method. A flask containing sodium hydride (3.90 g, 0.163 mol) suspended in anhydrous THF was cooled in an ice−water bath for 30 min. Pyrazole (11.3 g, 0.163 mol) was added over 15 min, and the resulting solution was allowed to stir at 0 °C for 30 min. Thionyl chloride (5.94 mL, 81.4 mmol) was added dropwise over 10 min. Once the addition was complete, the ice−water bath was removed, and the resulting suspension was allowed to warm to room temperature with stirring over 40 min, after which time isophthalaldehyde (2.73 g, 20.4 mmol) and anhydrous cobalt chloride (0.26 g, 2.0 mmol) were added at once, and the system was heated at reflux for 24 h. After cooling to room temperature, 160 mL of water was added and the resulting solution was stirred at room temperature for 30 min. The organic and aqueous layers were separated, and the aqueous layer was extracted with CH_2Cl_2 (2 × 100 mL). The combined organic extracts were washed with water (100 mL) and dried over $MgSO_4$. Removal of the solvent left a brown solid that was recrystallized from absolute ethanol to yield 5.06 g (67%) of **L*m*** that was pure by melting point (129−130 °C) and by NMR.

α,α,α′,α′-Tetra(1-pyrazolyl)-*p*-xylene, *p*-$[CH(pz)_2]_2C_6H_4$ (L*p*). CO(pz)$_2$ Method. Terephthaldicarboxaldehyde (0.50 g, 3.73 mmol), 1,1′-carbonyldipyrazole (1.21 g, 7.46 mmol), and anhydrous cobalt chloride (0.10 g, 0.77 mmol) were dissolved in 50 mL of anhydrous THF and heated at reflux for 21 h. After cooling to room temperature, 25 mL of distilled water was added, and the solution was stirred for 30 min and extracted with CH_2Cl_2 (3 × 25 mL). The combined organic extracts were washed with water (75 mL), concentrated NaCl solution (35 mL), and water (40 mL) and then dried over

(10) (a) Reger, D. L.; Semeniuc, R. F.; Rassolov, V.; Smith, M. D. *Inorg Chem.* **2004**, *43*, 537. (b) Reger, D. L.; Semeniuc, R. F.; Silaghi-Dumitrescu, I.; Smith, M. D. *Inorg Chem.* **2003**, *42*, 3751. (c) Reger, D. L.; Semeniuc, R. F.; Smith, M. D. *J. Chem. Soc., Dalton Trans.* **2003**, 285. (d) Reger, D. L.; Brown, K. J.; Smith, M. D. *J. Organomet. Chem.* **2002**, *658*, 50. (e) Reger, D. L.; Semeniuc, R. F.; Smith, M. D. *J. Chem. Soc., Dalton Trans.* **2002**, 476. (f) Reger, D. L.; Semeniuc, R. F.; Smith, M. D. *Inorg. Chem.* **2001**, *40*, 6545.

(11) (a) Khlobystov, A. N.; Blake, A. J.; Champness, N. R.; Lemenovskii, D. A.; Majouga, G.; Zyk, N. V.; Schroder, M. *Coord. Chem. Rev.* **2001**, *222*, 155. (b) Sénèque, O.; Giorgi, M.; Reinaud, O. *Chem. Commun.* **2001**, 984. (c) Weiss, H.-C.; Blaser, D.; Boese, R.; Doughan, B. M.; Haley, M. M. *Chem. Commun.* **1997**, 1703. (d) Madhavi, N. N. L.; Katz, A. K.; Carrell, H. L.; Nangia, A.; Desiraju, G. R. *Chem. Commun.* **1997**, 1953. (e) Jennings, W. B.; Farrell, B. M.; Malone, J. F. *Acc. Chem. Res.* **2001**, *34*, 885. (f) Calhorda, M. J. *Chem. Commun.* **2000**, 801. (g) Desiraju, G. R. *Acc. Chem. Res.* **1996**, *29*, 441. (h) Grepioni, F.; Cojazzi, G.; Draper, S. M.; Scully, N.; Braga, D. *Organometallics* **1998**, *17*, 296. (i) Weiss, H.-C.; Boese, R.; Smith, H. L.; Haley, M. M. *Chem. Commun.* **1997**, 2403. (j) Hunter, C. A.; Sanders, J. K. M. *J. Am. Chem. Soc.* **1990**, *112*, 5525. (k) Janiak, C. *J. Chem. Soc., Dalton Trans.* **2000**, 3885.

(12) Schmidt, S. P.; Trogler, W. C.; Basolo, F. *Inorg. Synth.* **1990**, *28*, 160.

(13) Casado Lacabra, M. A.; Canty, A. J.; Lutz, M.; Patel, J.; Spek, A. L.; Sun, H.; van Koten, G. *Inorg. Chim. Acta* **2002**, *327*, 15.

(14) Byers, P. K.; Canty, A. J.; Honeyman, R. T. *Inorg. Synth.* **2004**, *34*, 30.

$MgSO_4$. The solution was then concentrated and chromatographed (silica gel, acetone/hexanes, 1:1) to afford 0.920 g (67% yield) of a white solid. Mp: 165−166 °C. Anal. Calcd: C, 64.86; H, 4.90; N, 30.25. Found: C, 64.69; H, 4.76; N, 30.11. IR (KBr, cm^{-1}): 3130, 3109, 3011, 2942, 1516, 1434, 1413, 825, 792. ^1H NMR (300 MHz, $CDCl_3$): δ 7.71 (s, 2 H, C*H*(pz)$_2$), 7.62 (d, J = 1.2 Hz, 4 H, 5-H pz), 7.54 (d, J = 2.4 Hz, 4 H, 3-H pz), 7.02 (s, 4 H, C_6H_4), 6.33 (dd, J = 0.6, 2.0 Hz, 4 H, 4-H pz). ^{13}C NMR (100.6 MHz, acetone-d_6): δ 141.1, 139.1, 131.0, 128.2, 107.2, 77.8. HRMS: calcd for $C_{20}H_{18}N_8$, 370.1654; found 370.1644. Direct Probe MS *m/z* (rel int %) [assgn]: 370 (45) $[M]^+$, 303 (100) $[M - pz]^+$, 235 (30) $[M - pz - Hpz]^+$.

SO(pz)$_2$ Method. Sodium hydride (4.29 g, 0.179 mol) was suspended in 200 mL of THF and cooled in an ice−water bath for 30 min. Pyrazole (12.2 g, 0.179 mol) was added over 15 min, and the resulting solution was stirred at 0 °C for 30 min. Thionyl chloride (6.53 mL, 89.4 mmol) was added dropwise over 10 min at 0 °C, and the resulting pale yellow suspension was allowed to reach room temperature while stirring for 40 min. Terephthaldicarboxaldehyde (3.00 g, 22.4 mmol) and anhydrous cobalt chloride (0.29 g, 2.24 mmol) were added to this suspension at once, and the system was heated at reflux for 24 h. After cooling to room temperature, 160 mL of water was added and the system stirred for 30 min. The organic and aqueous layers were separated, and the aqueous layer was extracted with CH_2Cl_2 (2 × 100 mL). The combined organic extracts were washed with water (100 mL), dried over $MgSO_4$, and stripped, leaving a pale yellow solid that was recrystallized from absolute ethanol to afford 7.33 g (89%) of **L$_p$** that was pure by melting point (166−168 °C) and by NMR.

α,α,α′,α′-Tetrakis(4-benzylpyrazol-1-yl)-*p*-xylene, *p*-[CH(4Bnpz)$_2$]$_2$C$_6$H$_4$ (4BnL$_p$). Sodium hydride (0.607 g, 25.3 mmol) was suspended in 100 mL of THF and cooled in an ice−water bath. A 30 mL THF solution of 4-benzylpyrazole (4.00 g, 25.3 mmol) was added over 15 min, and the resulting solution was stirred at 0 °C for 30 min. Thionyl chloride (0.92 mL, 12.6 mmol) was added dropwise over 10 min at 0 °C, and the resulting pale yellow suspension was allowed to warm to room temperature while stirring for 40 min. Terephthaldicarboxaldehyde (0.424 g, 3.16 mmol) and $CoCl_2$ (0.082 g, 0.63 mmol) were added to this suspension at once, and the system was heated at reflux for 24 h. After cooling to room temperature, 100 mL of water was added and the system stirred for 45 min. The resulting solution was extracted with CH_2Cl_2 (1 × 100 mL, 2 × 70 mL), and the combined extracts were washed with water (100 mL) and dried over $MgSO_4$. Removal of the solvent afforded a red-brown oil that was taken up in CH_2Cl_2 and chromatographed (silica gel, Et_2O/CH_2Cl_2, 1:1) to yield 1.47 g (64%) of an off-white solid. Mp: 124−125 °C. Anal. Calcd for $C_{48}H_{42}N_8$: C, 78.88; H, 5.79; N, 15.33. Found: C, 78.66; H, 5.69; N, 15.24. IR (KBr, cm^{-1}): 3142, 3101, 3085, 3019, 2938, 2913, 1597, 1512, 1495, 1446, 768, 814, 694. ^1H NMR (400 MHz, acetone-d_6): δ 7.76 (s, 2 H, C*H*(^{4Bn}pz)$_2$), 7.60 (d, J = 0.8 Hz, 4 H, 5-H ^{4Bn}pz), 7.38 (s, 4 H, 3-H ^{4Bn}pz), 7.26−7.14 (m, 20 H, $CH_2C_6H_5$), 7.04 (s, 4 H, C_6H_4), 3.80 (s, 8 H, $CH_2C_6H_5$). ^1H NMR (400 MHz, DMSO-d_6): δ 7.89 (s, 2 H, C*H*(^{4Bn}pz)$_2$), 7.62 (s, 4 H, 5-H ^{4Bn}pz), 7.40 (s, 4 H, 3-H ^{4Bn}pz), 7.27−7.14 (m, 20 H, $CH_2C_6H_5$), 7.02 (s, 4 H, C_6H_4), 3.74 (s, 8 H, $CH_2C_6H_5$) ^{13}C NMR (75.5 MHz, acetone-d_6): δ 142.2, 141.0, 139.1, 129.4, 129.35, 129.31, 128.1, 126.9, 122.5, 77.9, 30.98. HRMS: calcd for $C_{48}H_{42}N_8$, 730.3582; found 730.3517. Direct Probe MS *m/z* (rel int %) [assgn]: 730 (15) $[M]^+$, 573 (75) $[M - {}^{4Bn}pz]^+$, 415 (30) $[M - {}^{4Bn}pz\text{-}H^{4Bn}pz]^+$, 158 (100) $[H^{4Bn}pz]^+$.

{*m*-[CH(pz)$_2$]$_2$C$_6$H$_4$}Re(CO)$_3$Br (1). $Re(CO)_5Br$ (0.400 g, 0.985 mmol) was dissolved in hot toluene (ca. 70 °C) and added gradually by cannula to a refluxing toluene solution of excess *m*-$[CH(pz)_2]_2C_6H_4$ (**L$_m$**) (1.00 g, 0.270 mmol). A precipitate was soon noticeable. After the addition was complete, the system was stirred at reflux for an additional 5 h. After cooling, the solvent was removed in vacuo to leave a discolored solid that was washed with CH_2Cl_2 (5 mL) and dissolved in ca. 4 mL of acetone. Crystals of pure **1** were grown by vapor diffusion of Et_2O into 1 mL solutions of the crude solid. Yield = 0.235 g (33%). Mp: 254−255 °C. Anal. Calcd for $C_{23}H_{18}BrN_8O_3Re$: C, 38.34; H, 2.52; N, 15.55. Found: C, 38.66; H, 2.29; N, 15.41. IR, $\nu_{C\equiv O}$ (KBr, cm^{-1}): 2018, 1916, 1887. ^1H NMR (400 MHz, acetone-d_6): δ 8.54 (s, 1 H, C*H*(pz)$_2$[Re]), 8.42 (dd, J = 2.6, 0.6 Hz, 2 H, 5-H pz[Re]), 8.10 (dd, J = 2.4, 0.8 Hz, 2 H, 3-H pz-[Re]), 7.86 (s, 1 H, C*H*(pz)$_2$), 7.73 (dd, J = 2.4, 0.8 Hz, 2 H, 5-H pz), 7.52 (dd, J = 2.0, 0.8 Hz, 2 H, 3-H pz), 7.42 (t, J = 7.8 Hz, 1 H, 5-H C_6H_4), 7.05 (d, J = 8.8 Hz, 1 H, 4-H C_6H_4), 6.69 (dd, J = 2.4, 2.4 Hz, 2 H, 4-H pz[Re]), 6.44 (d, J = 8.0 Hz, 1 H, 6-H C_6H_4), 6.32 (dd, J = 2.4, 1.8 Hz, 2 H, 4-H pz), 5.68 (s, 1 H, 2-H C_6H_4). HRMS: calcd for $C_{23}H_{18}BrN_8O_3Re$, 720.0226; found 720.0213. Direct Probe MS *m/z* (rel int %) [assgn]: 720 (5) $[M]^+$, 370 (3) $[\mathbf{L}_m]^+$, 302 (100) $[\mathbf{L}_m - Hpz]^+$, 235 (93) $[\mathbf{L}_m - Hpz - pz\ ]^+$.

{*μ-m*-[CH(pz)$_2$]$_2$C$_6$H$_4$}[Re(CO)$_3$Br][Pt(*p*-tolyl)$_2$] (2). {*μ*-*m*-$[CH(pz)_2]_2C_6H_4$}$Re(CO)_3Br$ (**1**) (0.10 g, 0.14 mmol) and $[Pt(p\text{-tolyl})_2(SEt_2)]_2$ (0.080 g, 0.086 mmol) were combined in a flask, and CH_2Cl_2 (15 mL) was added. Soon after stirring was begun, a precipitate formed. After stirring for 48 h at room temperature, the precipitate was isolated by filtration and dried under vacuum. Yield = 0.073 g (48%). Mp: 280 °C dec. Anal. Calcd for $C_{37}H_{32}BrN_8O_3PtRe$: C, 40.48; H, 2.94; N, 10.21. Found: C, 40.44; H, 2.63; N, 10.21. IR $\nu_{C\equiv O}$ (KBr, cm^{-1}): 2020, 1893. ^1H NMR (500 MHz, acetone-d_6): δ 8.47 (s, 1 H, C*H*(pz)$_2$-[Re]), 8.39 (dd, J = 0.4, 2.6 Hz, 2 H, 5-H pz[Pt], 8.26 (s, 1 H, C*H*(pz)$_2$[Pt]), 8.16 (d, J = 2.6 Hz, 2 H, 5-H pz[Re]), 8.05 (d, J = 2.3 Hz, 2 H, 3-H pz[Re]), 7.54 (t, J = 8.0 Hz, 1 H, 5-H C_6H_4), 7.38 (d, J = 2.2 Hz, 2 H, 3-H pz[Pt]), 6.92 (d, J = 7.9 Hz, J_{PtH} = 69 Hz, 4 H, 2,6-H Pt($C_6H_4CH_3$)), 6.78 (d, J = 7.7 Hz, 1 H, 4-H C_6H_4), 6.66 (d, J = 8.3 Hz, 1 H, 6-H C_6H_4), 6.62 (d, J = 7.7 Hz, 4 H, 3,5-H Pt($C_6H_4CH_3$)), 6.57 (t, J = 2.6 Hz, 2 H, 4-H pz[Re]), 6.50 (d, J = 2.5 Hz, 2 H, 4-H pz[Pt]), 4.97 (s, 1 H, 2-H C_6H_4), 2.10 (s, 6 H, Pt($C_6H_4CH_3$)). ESI(+) HRMS: calcd for $[C_{37}H_{32}BrKN_8O_3PtRe]^+$, 1133.0603; found 1133.0574. MS ESI (+) *m/z* (rel int %) [assgn]: 1097 (5) $[M - H]^+$, 1007 (20) $[M - C_7H_7]^+$, 721 (20) $[M - Pt(C_7H_7)_2]^+$, 641 (30) $[M - Pt(C_7H_7)_2 - CO - H]^+$, 303 (100) $[\mathbf{L}_m - pz]^+$.

{*μ-m*-[CH(pz)$_2$]$_2$C$_6$H$_4$}[Re(CO)$_3$Br]$_2$ (3). Toluene Method. $Re(CO)_5Br$ (0.900 g, 2.22 mmol) and *m*-$[CH(pz)_2]_2C_6H_4$ (**L$_m$**) (0.400 g, 1.08 mmol) were combined in a flask to which 50 mL of toluene was then added. Upon heating, the solids dissolved, and the solution was heated at reflux for 21 h, during which time a white precipitate formed. After cooling, the solvent was removed in vacuo, leaving an off-white solid that was chromatographed (silica gel, 1:9 to 3:7 acetone/Et_2O) to yield 0.58 g (50%) of pure **3**. Mp: 275 °C dec. Anal. Calcd for $C_{26}H_{18}Br_2N_8O_6Re_2$: C, 29.17; H, 1.69; N, 10.47. Found: C, 29.27; H, 1.52; N, 10.02. IR $\nu_{C\equiv O}$ (KBr, cm^{-1}): 2026, 1904. ^1H NMR (300 MHz, acetone-d_6): δ 8.55 (s, 2 H, C*H*(pz)$_2$), 8.41 (d, J = 2.4 Hz, 4 H, 5-H pz), 8.12 (d, J = 2.4 Hz, 4 H, 3-H pz), 7.47 (t, J = 8.0 Hz, 1 H, 2-H C_6H_4), 6.75 (t, J = 2.8 Hz, 4 H, 4-H pz), 6.67 (d, J = 8.8 Hz, 2 H, 4,6-H C_6H_4), 4.92 (s, 1 H, 2-H C_6H_4). Direct Probe MS *m/z* (rel int %) [assgn]: 1070 (1) $[M]^+$, 990 (1) $[M - Br]^+$, 962 (1) $[M - Br - CO]^+$, 934 (1) $[M - Br - 2CO]^+$, 906 (1) $[M - Br - 3CO]^+$, 720 (15) $[M - Re(CO)_3Br]^+$, 302 (100) $[\mathbf{L}_m - Hpz]^+$, 235 (99) $[\mathbf{L}_m - Hpz - pz]^+$.

Acetone Method. $Re(CO)_5Br$ (0.450 g, 1.11 mmol) and *m*-$[CH(pz)_2]_2C_6H_4$ (**L$_m$**) (0.200 g, 0.540 mmol) were dissolved in acetone, and the solution was heated at reflux for 2 days. Removal of the solvent after cooling yielded 0.50 g (87%) of **3**, whose ^1H NMR spectra suggested slight contamination with the monometallic complex.

{*μ-p*-[CH(pz)$_2$]$_2$C$_6$H$_4$}[Re(CO)$_3$Br]$_2$ (4). Toluene Method. $Re(CO)_5Br$ (0.22 g, 0.54 mmol) and *p*-$[CH(pz)_2]_2C_6H_4$ (**L$_p$**) (0.10 g, 0.27 mmol) were combined in a flask to which 40 mL of toluene was then added. Upon heating, the solids dissolved, and the solution was heated at reflux for 6 h. The precipitate that had formed was filtered and washed with 10 mL of toluene to yield 0.220 g (76% yield) of a white solid. Mp: 250

Table 1. Crystal Data and Refinement Details for {*m*-[CH(pz)$_2$]$_2$C$_6$H$_4$}Re(CO)$_3$Br (1), {*μ-m*-[CH(pz)$_2$]$_2$C$_6$H$_4$}[Re(CO)$_3$Br][Pt(*p*-tolyl)$_2$]·Et$_2$O (2·Et$_2$O), {*μ-m*-[CH(pz)$_2$]$_2$C$_6$H$_4$}[Re(CO)$_3$Br]$_2$·CH$_3$CN (3·CH$_3$CN), {*μ-p*-[CH(pz)$_2$]$_2$C$_6$H$_4$}[Re(CO)$_3$Br]$_2$·3C$_3$H$_6$O (4·3C$_3$H$_6$O), and {*μ-p*-[CH(4Bnpz)$_2$]$_2$C$_6$H$_4$}[Re(CO)$_3$Br]$_2$·Et$_2$O·4DMSO (5·Et$_2$O·4DMSO)

	1	**2**·Et$_2$O	**3**·CH$_3$CN	**4**·3C$_3$H$_6$O	**5**·Et$_2$O·4DMSO
empirical formula	$C_{23}H_{18}BrN_8O_3Re$	$C_{41}H_{42}BrN_8O_4PtRe$	$C_{28}H_{21}Br_2N_9O_6Re_2$	$C_{35}H_{36}Br_2N_8O_9Re_2$	$C_{66}H_{76}Br_2N_8O_{11}Re_2S_4$
fw	720.56	1172.03	1111.76	1244.94	1817.81
T (K)	293(1)	150(1)	200(1)	150(1)	150(1)
cryst syst	monoclinic	monoclinic	triclinic	monoclinic	triclinic
space group	$P2_1/n$	$P2_1/c$	$P\bar{1}$	$C2/c$	$P\bar{1}$
a, Å	8.1445(4)	15.5427(7)	11.3267(18)	18.5053(11)	11.9047(6)
b, Å	20.6300(11)	15.3800(7)	13.334(2)	14.6677(9)	12.4073(7)
c, Å	15.6330(8)	18.8150(9)	14.442(2)	15.6163(10)	13.0787(7)
α, deg	90	90	108.914(3)	90	92.3880(10)
β, deg	104.5000(10)	112.0780(10)	93.987(3)	92.034(2)	90.2820(10)
γ, deg	90	90	108.683(3)	90	112.0980(10)
V, Å^3	2543.0(2)	4167.9(3)	1917.8(5)	4236.1(5)	1787.89(17)
Z	4	4	2	4	1
D(calc), Mg·m^{-3}	1.882	1.868	1.925	1.952	1.688
abs coeff, mm^{-1}	6.391	7.264	8.437	7.656	4.679
cryst size, mm^3	0.28 × 0.20 × 0.16	0.14 × 0.10 × 0.08	0.38 × 0.18 × 0.14	0.16 × 0.08 × 0.06	0.40 × 0.28 × 0.14
final R indices [$I > 2\sigma(I)$]					
R1	0.0267	0.0313	0.0366	0.0469	0.0243
wR2	0.0642	0.0697	0.0851	0.1065	0.0617

°C dec. Anal. Calcd for $C_{26}H_{18}Br_2N_8O_6Re_2$: C, 29.17; H, 1.69; N, 10.47. Found: C, 28.75; H, 1.75; N, 10.41. IR $\nu_{C\equiv O}$ (KBr, cm^{-1}): 2018, 1900. ^{1}H NMR (300 MHz, acetone-d_6): δ 8.59 (s, 2 H, C*H*(pz)$_2$), 8.45 (dd, J = 2.7, 0.6 Hz, 4 H, 5-H pz), 8.16 (d, J = 1.8 Hz, 4 H, 3-H pz), 6.74 (t, J = 2.6 Hz, 4 H, 4-H pz), 6.43 (s, 4 H, C$_6$*H*$_4$). ESI(+) HRMS calcd for $C_{26}H_{18}Br_2KN_8O_6Re_2$, 1108.8429; found 1108.8461. MS ESI(+) *m/z* (rel int %) [assgn]: 1109 (40) [M + K]$^+$, 991 (100) [M − Br]$^+$, 720 (5) [M − Re(CO)$_3$Br]$^+$, 641 (5) [M − Re(CO)$_3$Br − Br]$^+$, 614 (10) [M − Re(CO)$_3$Br − Br − CO]$^+$.

Acetone Method. Re(CO)$_5$Br (0.450 g, 1.11 mmol) and *p*-[CH(pz)$_2$]$_2$C$_6$H$_4$ (**L*p***) (0.200 g, 0.540 mmol) were dissolved in acetone, and the solution was heated at reflux for 70 h, by which time a white precipitate had formed. After cooling to room temperature, the precipitate was isolated by cannula filtration, washed with acetone (2 × 20 mL), and dried in vacuo. The precipitate was found to be pure **4**. Yield = 0.164 g (57%).

{*μ-p*-[CH(pz^{4Bn})$_2$]$_2$C$_6$H$_4$}[Re(CO)$_3$Br]$_2$ (5). Re(CO)$_5$Br (0.23 g, 0.57 mmol) and *p*-[CH(pz^{4Bn})$_2$]$_2$C$_6$H$_4$ (**^{4Bn}L*p***) (**7**) (0.20 g, 0.27 mmol) were combined in a flask to which 50 mL of toluene was added, and the system was heated at reflux for 5 h, during which time a white precipitate formed. After cooling to room temperature, the solid was isolated by cannula filtration, washed with acetone (5 mL), and dried in vacuo to yield 0.285 g (71%) of a white solid. Mp: 296 °C dec. Anal. Calcd for $C_{54}H_{42}Br_2N_8O_6Re_2$: C, 45.32; H, 2.96; N, 7.83. Found: C, 45.61; H, 2.99; N, 7.52. IR $\nu_{C\equiv O}$ (KBr, cm^{-1}): 2022, 1912, 1896. ^{1}H NMR (400 MHz, DMSO-d_6): δ 8.49, (s, 2 H, C*H*(4-Bnpz)$_2$), 8.16 (s, 4 H, 5-H 4-Bnpz), 7.97 (s, 4 H, 3-H 4-Bnpz), 7.34−7.21 (m, 20 H, CH$_2$C$_6$*H*$_5$), 6.21 (s, 4 H, C$_6$*H*$_4$), 3.91 (dd, J = 20, 16 Hz, 8 H, C*H*$_2$C$_6$H$_5$).

Crystal Structure Determinations. X-ray intensity data from colorless blocks of **1**, **2**, and **5**, a colorless prism of **3**, and an irregular colorless crystal of **4** were measured at 150(1) K for **2**, **4**, and **5**, at 293(1) K for **1**, and at 200(1) K for **3** on a Bruker SMART APEX CCD-based diffractometer (Mo Kα radiation, λ = 0.71073 Å).[15] All crystals were taken directly from the crystallizing container. Raw data frame integration and *Lp* corrections were performed with SAINT+.[15] Final unit cell parameters were determined by least-squares refinement of 6699, 7111, 7862, 5660, and 8246 reflections from the data sets of **1**−**5**, respectively, each with $I > 5\sigma(I)$. Analysis of the data showed negligible crystal decay during data collection. An empirical absorption correction was applied with SADABS.[15] Patterson (for **1**) or direct (for **2**−**5**) methods structure solution, difference Fourier calculations, and full-matrix least-squares refinement against F^2 were performed with SHELXTL.[16] Hydrogen atoms for all species were placed in geometrically idealized positions and included as riding atoms. Details of the data collections are given in Table 1 while further notes regarding the solution and refinement for **1**−**5** follow.

Systematic absences in the intensity data for compound **1** confirmed the space group $P2_1/n$. The asymmetric unit consists of a complete molecule of the monometallic complex.

For compound **2**, systematic absences in the intensity data were consistent with the space group $P2_1/c$. All non-hydrogen atoms of the metal complex were refined with anisotropic displacement parameters. The metal complex crystallizes with one badly disordered diethyl ether molecule per complex. The Et$_2$O was modeled as being statistically disordered over three independent sites in the asymmetric unit and was refined with the aid of 22 distance restraints. Each disorder component was assigned a common isotropic displacement parameter.

Compound **3** crystallizes in the triclinic system. The space group $P\bar{1}$ was assumed and confirmed by successful solution and refinement of the data. Location and anisotropic refinement of the Re complex proceeded without incident. Another region of electron density in the near vicinity of the Re complex was successfully modeled as an acetonitrile molecule of crystallization disordered over three positions. Atoms of the acetonitrile were refined isotropically subject to a total of six distance restraints. The acetonitrile nitrogen atom occupies a site common to all three disorder components. Another region of electron density assumed to be severely disordered solvent species was also observed in channels running parallel to the crystallographic *a*-axis. This could not be modeled successfully and was treated with the SQUEEZE routine in PLATON.[17] The program calculated a solvent-accessible void volume of 276.2 Å^3, corresponding to 64 e$^-$/cell. The contribution of these diffusely scattering species was removed from subsequent structure factor calculations. The final reported F(000), MW, and calculated density reflect the identified species only.

(15) *SMART* Version 5.625, *SAINT*+ Version 6.22, and *SADABS* Version 2.05; Bruker Analytical X-ray Systems, Inc.: Madison, WI, 2001.

(16) Sheldrick, G. M. *SHELXTL* Version 6.1; Bruker Analytical X-ray Systems, Inc.: Madison, WI, 2000.

(17) *PLATON*: (a) Spek, A. L. *Acta Crystallogr., Sect. A* **1990**, *46*, C34. (b) Spek, A. L. *PLATON*, A Multipurpose Crystallographic Tool; Utrecht University: Utrecht, The Netherlands, 2002.

Scheme 1

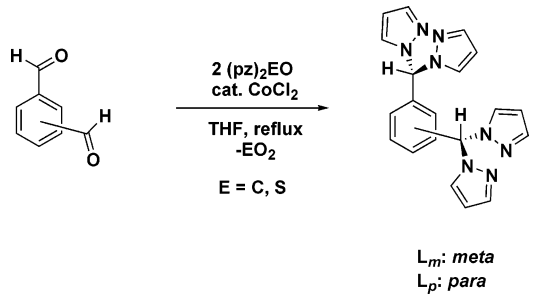

Systematic absences in the intensity data of compound **4** were consistent with either of the space groups *C*2/*c* or *Cc*; the former was eventually confirmed. The asymmetric unit consists of half of the $[(ReBr(CO)_3)_2(\mu\text{-}C_{20}H_{18}N_8)]$ complex on a center of symmetry along with one complete acetone and half of another acetone located on a C_2 axis.

Compound **5** crystallizes in the triclinic system. The space group $P\bar{1}$ was assumed and confirmed by the successful solution and refinement of the data. The asymmetric unit consists of half a $[((CO)_3ReBr)_2(\mu\text{-}C_{48}H_{42}N_8)]$ complex located on an inversion center, half an Et_2O molecule of crystallization that is disordered about an inversion center, and two independent DMSO molecules of crystallization. One of the DMSO molecules (S2) is disordered, and a restrained model employing two orientations in the ratio 0.75 (S2A):0.25 (S2B) was refined. The geometry of the disordered DMSO was restrained to be similar to that of the ordered DMSO (12 restraints, SHELX SAME). All non-hydrogen atoms were refined with anisotropic displacement parameters except the carbon and oxygen atoms of the disordered DMSO (isotropic).

Results and Discussion

Syntheses. The ligands *m*- and *p*-$C_6H_4[CH(pz)_2]_2$ ($\mathbf{L}_m$ and $\mathbf{L}_p$, respectively) were prepared as shown in Scheme 1 by the cobalt-catalyzed condensation reaction, first reported by Peterson,[18] between the respective dicarboxaldehyde and $EO(pz)_2$ (E = C or S). Although the reagent $CO(pz)_2$ is sometimes preferred in this reaction because of greater reactivity,[18b] we have found that $SO(pz)_2$, prepared in situ from sodium pyrazolate and thionyl chloride, gives higher yields and requires simpler workup procedures with many of our systems.[19] The additional advantage of avoiding the use of phosgene, from which $CO(pz)_2$ is prepared,[14] is clear. The $CO(pz)_2$ route, therefore, was ultimately abandoned, and the ligand *p*-$C_6H_4[CH(^{4Bn}pz)_2]_2$ ($^{4Bn}\mathbf{L}_p$; ^{4Bn}pz = 4-benzyl-1-pyrazolyl) was synthesized only by using $SO(^{4Bn}pz)_2$.

Each ligand is air stable and freely soluble in halogenated solvents, acetone, and toluene but only moderately soluble in diethyl ether and acetonitrile. When using the $SO(pz)_2$ route, they may be obtained analytically pure after workup by recrystallization of the crude solid from boiling absolute ethanol.

The monometallic rhenium complex of $\mathbf{L}_m$, {*m*-[CH-$(pz)_2]_2C_6H_4$}$Re(CO)_3Br$ (**1**), could be prepared by reacting equimolar amounts of the ligand and $Re(CO)_5Br$ in either toluene or acetone, but the product also contained significant amounts of the bimetallic rhenium complex {μ-*m*-$[CH(pz)_2]_2C_6H_4$}$[Re(CO)_3Br]_2$ (**3**). The separation of the two species by column or preparative thin-layer chromatography was impractical on a useful scale. Instead, the most reliable method of obtaining the monometallic species analytically pure was by selectively crystallizing it through vapor diffusion of diethyl ether into acetone solutions of the mixture. Interestingly, although the two species possessed almost identical R_f values in the solvent systems tested, their solubility in acetone/ether was distinct such that **1** was the only species to crystallize within 1−2 weeks. Nevertheless, when starting from equimolar amounts of the reactants, the final yield of **1** was extremely low because of the significant amounts of the bimetallic species concomitantly formed. A modified procedure, therefore, was developed in which the formation of the unwanted species was minimized (Scheme 2). Thus, slow addition of a hot toluene solution of $Re(CO)_5Br$ to a refluxing solution of excess $\mathbf{L}_m$ reduced the level of **3** formed almost to the limit of detection by ^{1}H NMR.

It is worth noting that a similar route was also attempted in which $Re(CO)_3(THF)_2Br$ was prepared by heating $Re(CO)_5Br$ in THF at reflux according to a report by Storhoff and Lewis.[20] Unfortunately, after several trials, the reaction of this adduct failed to yield the desired complex.

The corresponding monometallic rhenium complex of $\mathbf{L}_p$ could not be prepared. The solubilities of the complexes of the *p*-phenylene-linked ligands used in this work were relatively low, likely preventing the isolation of the monometallic complex.

A suspension of **1** in CH_2Cl_2 at room temperature slowly reacted with dissolved $[Pt(SEt_2)(p\text{-tolyl})_2]_2$ to yield the heterobimetallic complex {μ-*m*-$[CH(pz)_2]_2C_6H_4$}-$[Re(CO)_3Br][Pt(p\text{-tolyl})_2]$, **2** (Scheme 2). We chose the organometallic Pt(II) unit $[Pt(p\text{-tolyl})_2]$ because of the ease with which it could be introduced into the complex via the dimer $[Pt(SEt_2)(p\text{-tolyl})_2]_2$[13] and because of the known unusual photochemical properties of related complexes.[21] Complex **2** was insoluble in CH_2Cl_2 and could be isolated analytically pure by filtration. The complex could be redissolved in acetone.

The bimetallic rhenium complex of $\mathbf{L}_m$, {μ-*m*-[CH-$(pz)_2]_2C_6H_4$}$[Re(CO)_3Br]_2$ (**3**), as mentioned above, was formed in significant amounts in the equimolar reaction of $Re(CO)_5Br$ and $\mathbf{L}_m$. The complex was formed exclusively when 2 equiv of $Re(CO)_5Br$ was used in the reaction. The corresponding complex of $\mathbf{L}_p$, {μ-*p*-[CH-$(pz)_2]_2C_6H_4$}$[Re(CO)_3Br]_2$ (**4**), was prepared by the same route (Scheme 3). The reactions could be carried out in toluene or in acetone. $Re(CO)_5Br$ is insoluble in toluene at room temperature but does dissolve at higher temperatures. Shortly after its complete dissolution in the presence of ligand, a precipitate formed, and after several hours, the homobimetallic complexes were isolated by filtration from the supernatant, in which they were completely insoluble. Alternatively, either ligand and $Re(CO)_5Br$ could be dissolved in acetone at room

(18) (a) Thé, K. I.; Peterson, L. K. *Can. J. Chem.* **1973**, *51*, 422. (b) Thé, K. I.; Peterson, L. K.; Kiehlman, E. *Can. J. Chem.* **1973**, *51*, 2448. (c) Peterson, L. K.; Kiehlman, E.; Sanger, A. R.; Thé, K. I. *Can. J. Chem.* **1974**, *52*, 2367.

(19) Reger, D. L.; Grattan, T. C.; Brown, K. J.; Little, C. A.; Lamba, J. J. S.; Rheingold, A. L.; Sommer, R. D. *J. Organomet. Chem.* **2000**, *607*, 120.

(20) Storhoff, B. N.; Lewis, H. C. *Synth. React. Inorg. Metal-Org. Chem.* **1974**, *4*, 467.

(21) (a) Wadas, T. J.; Lachicotte, R. J.; Eisenberg, R. *Inorg. Chem.* **2003**, *42*, 3772. (b) Hissler, M.; McGarrah, J. E.; Connick, W. B.; Geiger, D. K.; Cummings, S. D.; Eisenberg, R. *Coord. Chem. Rev.* **2000**, *208*, 115.

Scheme 2

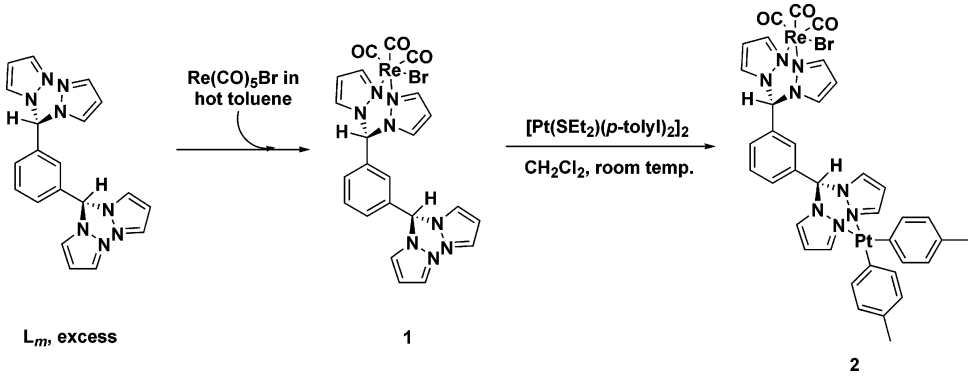

Scheme 3

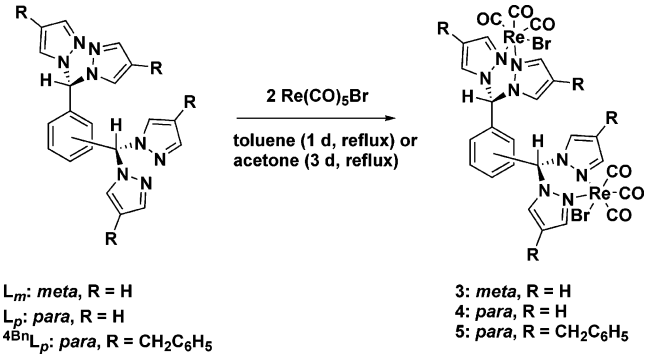

temperature and heated at reflux for 3 days to yield the respective complex. Despite the longer reaction time, the latter method was preferred because it was easier to monitor by NMR. Complex **3** did not precipitate from acetone, but some precipitate of **4** was observed. The addition of more acetone redissolved the product.

The reaction of 2 equiv of $Re(CO)_5Br$ with p-C_6H_4-$[CH(^{4Bn}pz)_2]_2$ ($^{4Bn}\mathbf{L}_p$) in refluxing toluene yielded $\{\mu$-p-$[CH(pz^{4Bn})_2]_2C_6H_4\}[Re(CO)_3Br]_2$ (**5**) (Scheme 3). Although pendent benzyl groups might have improved solubility through increased interactions with solvents, **5** was considerably *less* soluble than the corresponding underivatized compound and could be dissolved only in dimethyl sulfoxide. It was also insufficiently volatile to yield useful mass spectral characterization. As shown below, the pendent benzyl group introduced new types of noncovalent intermolecular forces to the supramolecular structure.

IR, NMR, and Mass Spectral Characterization. The IR spectrum of each complex displays the characteristic ν(C≡O) absorbances at ca. 2000 (sharp) and 1900 (broad) cm^{-1}, which are indicative of local C_{3v} symmetry and consistent with facial coordination of the CO ligands. The ^1H NMR spectra of the homobimetallic complexes **3**−**5** each show equivalent pyrazolyl rings indicating free rotation at room temperature of the bis(pyrazolyl)methane group about the bond joining it to the linking phenylene ring. The ^1H NMR spectrum of **1** shows the nonequivalence of the coordinated and uncoordinated bis(pyrazolyl)methane units of the ligand, as expected. The uncoordinated bis(pyrazolyl)methane site in **1** has resonances nearly identical to those of the free ligand, whereas the resonances of the coordinated site are all shifted significantly downfield. For example, the methine, 5-pyrazolyl, and 3-pyrazolyl protons resonate at 7.86, 7.73, and 7.52 ppm, respectively, at the uncoordinated site compared with 7.93, 7.76, and 7.53 ppm for the free ligand, but the corresponding resonances of the coordinated site are at 8.54, 8.42, and 8.10 ppm. Similarly, each homobimetallic complex yielded symmetric spectra where the pyrazolyl ring resonances were shifted downfield from those of the respective free ligands.

The ^1H NMR spectrum of the heterobimetallic complex **2** could not be readily assigned because the resonances of the pyrazolyl groups for the rhenium and platinum ends of the molecule overlapped. A combination of correlation and NOE difference spectroscopy was used to make the assignments shown in Figure 1. The downfield region, which excludes the aryl proton H_N at 4.97 ppm and the tolyl methyl protons at 2.10 ppm, is shown. The signals from the pyrazolyl groups bound to Re are in the same regions as they are in the other Re complexes. The 5- and 3-pyrazolyl protons of the groups bound to Pt, however, are widely separated (8.40 and 7.37 ppm, respectively). In fact, the 5-pyrazolyl protons associated with the Pt center, H_B, are perturbed to such an extent that they resonate at a lower field than does the respective methine proton (8.27 ppm), a feature unique among the complexes described in this work. Furthermore, the 3-pyrazolyl protons, H_G, display a rather drastic shift upfield compared to the other complexes. The latter observation may be explained by the fact that these protons are likely within the shielding regions of the tolyl groups bound to Pt, a contention that is supported by the solid-state structure discussed below. The $^{195}Pt-^1H$ coupling satellites are located about the aryl doublet (H_H) at 6.92 ppm.

Another interesting feature of the spectrum of each complex is the dramatic upfield shift of the phenylene protons closest to the pyrazolyl rings. In the *meta*-phenylene-linked complexes, the most dramatic effects are observed with the proton that is *ortho* to both substituted carbon atoms of the central linker, e.g., H_N in the structure inset of Figure 1. For the *para*-phenylene-linked complexes, the aromatic protons on the central ring are all equivalent and *ortho* to one substituted ring carbon atom. Table 2 compares the chemical shifts of these protons in the complexes with those in the free ligands. The shielding effects are greatest for the single 2-hydrogen atom in $\mathbf{L}_m$ and are larger for the bimetallic complexes **2** and **3** than for the monometallic **1**. Less dramatic shielding effects in the complexes of $\mathbf{L}_m$ of ca. 0.3 ppm are observed with the 4- and 6-hydrogen atoms that are adjacent to only one substituent. The upfield shifts are likely caused by the

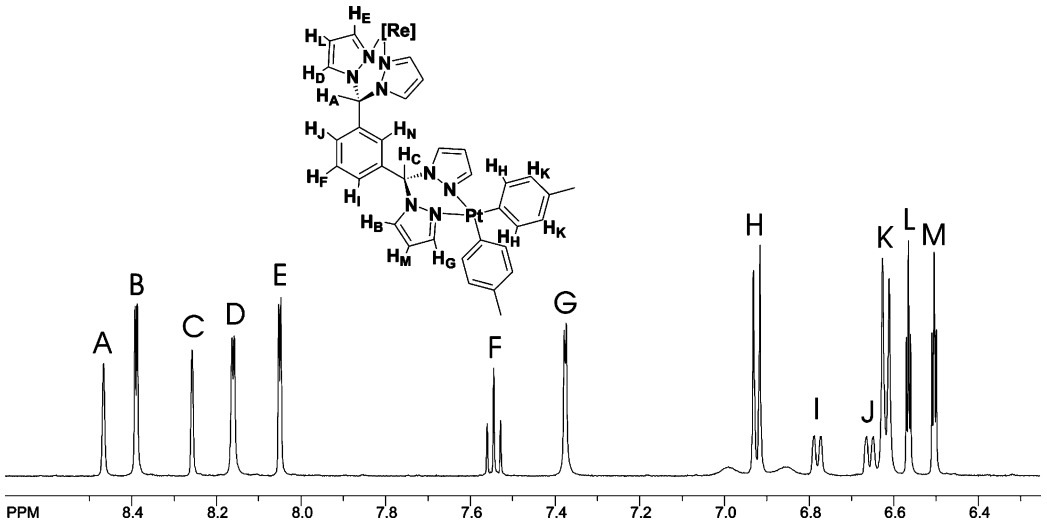

Figure 1. Downfield region of ^{1}H NMR spectrum of {μ-*m*-[CH(pz)$_2$]$_2$C$_6$H$_4$}[Re(CO)$_3$Br][Pt(*p*-tolyl)$_2$] (**2**) (500 MHz, acetone-d_6) showing peak assignments.

Table 2. ^{1}H NMR Data (ppm) for L$_m$, L$_p$, and 1−5

compound	phenylene 2-H[a]	phenylene 4-, 6-H
L$_m$	6.80	7.08
1	5.68	7.05, 6.44
2	4.97	6.78, 6.66
3	4.92	6.67
L$_p$	7.08	
4	6.43	
^{4Bn}L$_p$	7.04	
5	6.21	

[a] In the *meta*-phenylene-linked compounds, the proton *ortho* to both substituted aromatic carbons atoms. In the *para*-phenylene-linked compounds, all phenylene protons are equivalent.

positions of the protons in the shielding regions of coordinated pyrazolyl rings (vide infra).

The mass spectrum of the monometallic complex **1** includes a weak peak corresponding to the molecular ion as well as fragmentation peaks. The spectrum of the heterobimetallic complex **2** shows loss of a tolyl substituent at platinum as well as loss of the [Pt(*p*-tolyl)$_2$] unit itself. Spectra of the homobimetallic complexes **3** and **4** are somewhat more detailed and contain fragment peaks indicating sequential loss of Br and CO as well as [Re(CO)$_3$Br]. As mentioned above, the benzyl-substituted derivative **5** was insufficiently volatile for mass spectrometric analysis.

Solid-State Structures. The details of the crystallographic analysis of the ligand *m*-[CH(pz)$_2$]$_2$C$_6$H$_4$}, **L$_m$**, including a description of its supramolecular structure, are given in the Supporting Information.

An ORTEP diagram of {*m*-[CH(pz)$_2$]$_2$C$_6$H$_4$}Re(CO)$_3$-Br (**1**) is shown in Figure 2, and selected bond distances and angles are given in Table 3. In contrast to the other complexes in this study, the two bis(pyrazolyl)methane sites of **1** are both oriented on the same side of the connecting phenylene ring. One of the carbonyl ligands attached to the Re center is positioned directly over the central phenylene ring and is participating in $\pi\cdots\pi$ interactions. This feature is found in each of the complexes of this study, and its implications are discussed below.

Another important feature is an intramolecular CH$\cdots\pi$ interaction between H(8) and the nearby pyrazolyl rings containing C(11) and C(41). These 2.77 Å interactions with C(8)−H(8)$\cdots$Ct (Ct = centroid) angles of approximately 120° support the assumption made earlier that the shielding of H(8) noticed in the NMR spectrum is due to its proximity to the π clouds of these pyrazolyl rings. Similarly, the upfield shifts of the 4- and 6-protons (H(4) and H(6), respectively) on the linking phenylene ring can be explained by noting the ca. 3.0 Å interactions between these protons and the pyrazolyl rings containing N(21) and N(31). In contrast to H(8), H(4) and H(6) are each exposed to only one shielding pyrazolyl region and are at greater distances from these regions, thus explaining the smaller magnitude of the shielding.

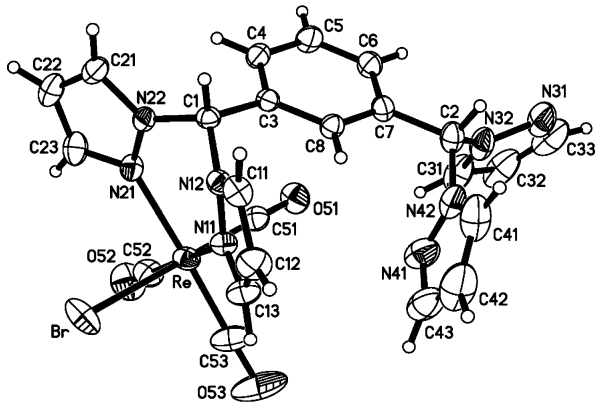

Figure 2. ORTEP drawing of {*m*-[CH(pz)$_2$]$_2$C$_6$H$_4$}Re(CO)$_3$-Br (**1**). Displacement ellipsoids are drawn at 30% probability.

The extended structure of **1** consists of sheets in the *bc*-plane that stack along the *a*-axis with no appreciable interactions between the planes. The planes are composed of chains of molecules along the *b*-axis (Figure 3, top) held together by pyrazolyl embrace interactions in which the CH$\cdots$Ct interactions are edge-to-face in orientation. The two protons interacting with the C(41)-containing pyrazolyl ring are H(21), at a distance of 3.04 Å and C(21)−H(21)$\cdots$Ct angle of 128°, and H(22), at a distance of 3.37 Å and C(22)−H(22)$\cdots$Ct angle of 113°. Similarly, H(32) is 3.74 Å from the C(11)-containing pyrazolyl ring with a C(32)−H(32)$\cdots$Ct angle of 114°, and H(33) is 3.81 Å from the same ring with a C(33)−

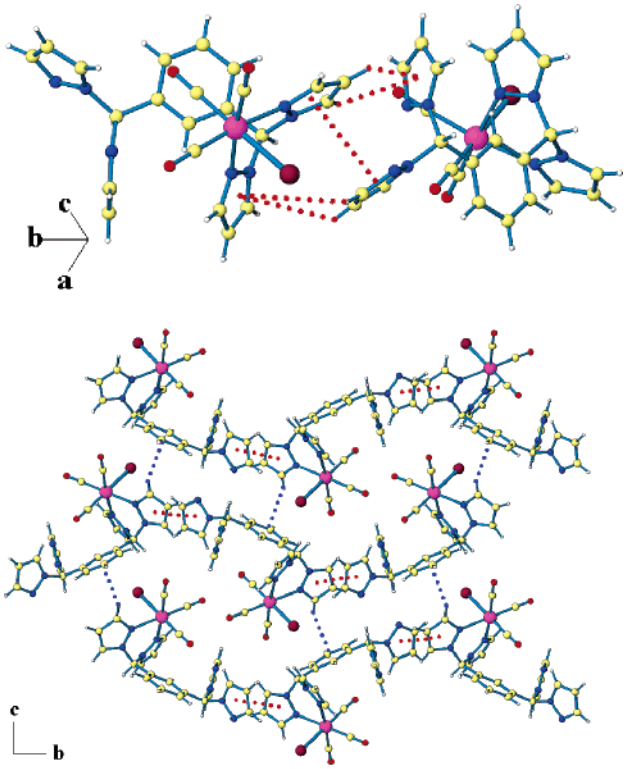

Figure 3. Views of **1** showing the pyrazolyl embrace (top) and sheets in the *bc*-plane (bottom). Pyrazolyl embrace interactions are shown in red; other CH···π interactions are in blue.

Table 3. Selected Bond Distances (Å) and Angles (deg) for 1, 2·Et$_2$O, and 3·CH$_3$CN

	1	**2**·Et$_2$O	**3**·CH$_3$CN
Re(1)−N(11)	2.171(3)	2.184(4)	2.173(5)
Re(1)−N(21)	2.177(3)	2.183(4)	2.174(5)
Re(2)−N(31)			2.184(6)
Re(2)−N(41)			2.167(5)
Re(1)−Br(1)	2.6208(5)	2.6201(6)	2.6330(8)
Re(2)−Br(2)			2.6313(8)
Re(1)−C(51)	1.898(4)		1.904(8)
Re(1)−C(52)	1.907(4)		1.912(8)
Re(1)−C(53)	1.896(4)		1.889(7)
Re(1)−C(71)		1.910(7)	
Re(1)−C(72)		1.909(6)	
Re(1)−C(73)		1.912(6)	
Pt(1)−N(31)		2.098(4)	
Pt(1)−N(41)		2.115(4)	
Pt(1)−C(51)		1.994(5)	
Pt(1)−C(61)		1.991(5)	
N(11)−Re(1)−N(21)	83.78(10)		84.06(19)
N(11)−Re(1)−Br(1)	82.99(8)		83.92(13)
C(51)−Re(1)−N(11)	97.43(13)		174.9(2)
C(53)−Re(1)−N(11)	91.73(17)		97.4(2)
C(51)−Re(1)−Br(1)	179.38(11)		92.5(2)
N(31)−Re(2)−N(41)			84.66(19)
N(31)−Re(2)−Br(2)			84.90(13)
C(61)−Re(2)−N(31)			174.1(3)
C(63)−Re(2)−N(31)			96.3(3)
C(61)−Re(2)−Br(2)			90.3(2)
C(61)−Pt(1)−C(51)		93.1(2)	
C(51)−Pt(1)−N(31)		173.7(2)	
C(61)−Pt(1)−N(31)		91.62(19)	
C(61)−Pt(1)−N(41)		174.9(2)	
C(51)−Pt(1)−N(41)		88.34(18)	
N(31)−Pt(1)−N(41)		87.34(16)	
C(72)−Re(1)−C(71)		89.6(3)	
C(71)−Re(1)−C(73)		87.7(2)	

H(33)···Ct angle of 113°. The centroids of the pyrazolyl rings containing C(21) and C(31) are 3.88 Å apart with a perpendicular distance of 3.56 Å (slip angle β = 23.12°). A recent survey of pyrazolyl embrace parameters for known bis(pyrazolyl)methane complexes[7b] revealed an average CH···centroid distance of 2.76 Å, an average corresponding angle of 142°, and an average centroid−centroid distance of 3.71 Å. Thus, the CH··· Ct parameters for complex **1** indicate a relatively weak pyrazolyl embrace.

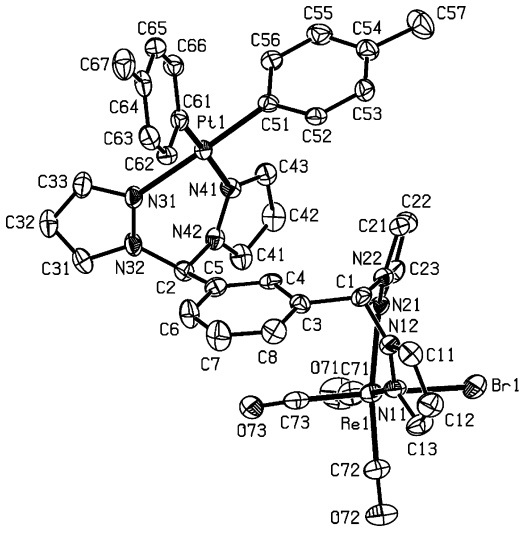

Figure 4. ORTEP drawing of the heterobimetallic molecule of {μ-*m*-[CH(pz)$_2$]$_2$C$_6$H$_4$}[Re(CO)$_3$Br][Pt(*p*-tolyl)$_2$]·Et$_2$O (**2**·Et$_2$O). Displacement ellipsoids drawn at the 50% probability level. Hydrogen atoms are omitted.

Each chain along the *b*-axis is bound to two adjacent chains by an interaction between H(23), at the 3-pyrazolyl position of the coordinated bis(pyrazolyl)methane site, and the π cloud of the *meta*-phenylene linker, thus completing the sheets in the *bc*-plane (Figure 3, bottom).

An ORTEP diagram showing the heterobimetallic molecule of {μ-*m*-[CH(pz)$_2$]$_2$C$_6$H$_4$}[Re(CO)$_3$Br][Pt(*p*-tolyl)$_2$]·Et$_2$O (**2**·Et$_2$O) is shown in Figure 4. Selected bond distances and angles are given in Table 3. As observed in all of the bimetallic complexes prepared here, the metal units are oriented on opposite sides of the linking phenylene group, with one carbonyl ligand attached to the Re center positioned over the central phenylene ring. There are two noncovalent intramolecular interactions of note. First, the CH···π interactions between H(4) and the pyrazolyl rings containing C(21) and C(41) explain the shielding of this proton in the NMR spectrum. Second, another intramolecular CH···π interaction between H(43) and the C(51)-containing tolyl ring bound to platinum explains the analogous shielding of H(43) in the NMR spectrum.

Significant noncovalent interactions extend the solid-state structure of **2**·Et$_2$O into all three dimensions. The basic unit is a dimer held together by reciprocal CH···π interactions, which include a 2.98 Å interaction between the methine hydrogen atom H(1) associated with the Re center and the tolyl ring containing C(51) (Figure 5, red dashed lines) and a 2.97 Å interaction between the 5-pz proton H(11) associated with Re and the same tolyl group (not pictured). The other 5-pz hydrogen atom of the Re side is weakly bound to the other tolyl group of the same Pt atom at a distance of 2.85 Å (Figure 5, red dashed lines). Each dimeric unit is interacting with two adjacent dimers along the *b*-axis via 2.77 Å CH···π

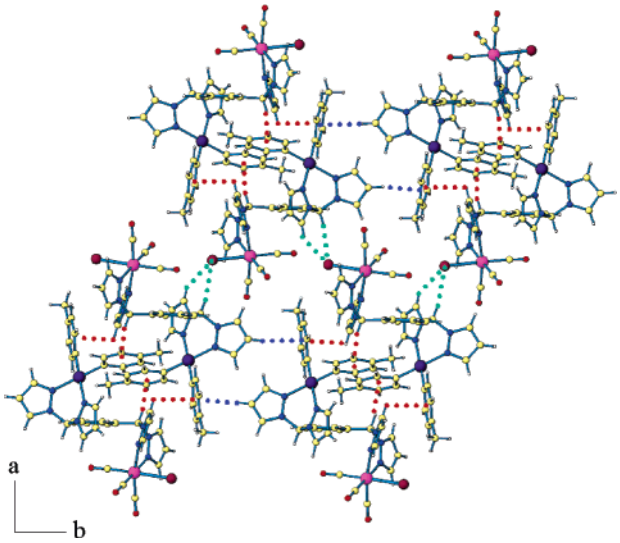

Figure 5. View of **2**·Et_2O showing sheets in the *ab*-plane formed from CH···π (red and blue dashed lines) and CH···Br (green dashed lines) noncovalent interactions. Solvent molecules are omitted.

bonds from the 4-pz hydrogen on the Pt side to an adjacent tolyl ring containing C(61) (Figure 5, blue dashed lines). These chains along the *b*-axis are extended into sheets by CH···Br hydrogen bonds between both the methine and 5-pz hydrogens on the Pt side and Br atoms on adjacent dimers in the *ab*-plane (Figure 5, green dashed lines). Finally, these sheets stack on one another along the *c*-axis by weak CH···O bonds between a 4-pz hydrogen atom on the Re side and a CO ligand in a molecule belonging to an adjacent sheet, thus completing the three-dimensional supramolecular structure of **2**·Et_2O.

Table 4. Selected Bond Distances (Å) and Angles (deg) for 4·3C_3H_6O and 5·Et_2O·4DMSO

	4·3C_3H_6O	**5**·Et_2O·4DMSO
Re(1)−N(11)	2.164(7)	2.186(2)
Re(1)−N(21)	2.184(6)	2.178(2)
Re(1)− C(31)	1.869(11)	1.912(3)
Re(1)−C(33)	1.908(9)	1.912(3)
Re(1)−C(32)	1.923(9)	1.913(3)
Re(1)−Br(1)	2.6363(9)	2.6428(3)
C(31)−O(31)	1.178(11)	1.153(4)
C(32)−O(32)	1.147(10)	1.154(4)
C(33)−O(33)	1.140(9)	1.136(4)
C(31)−Re(1)−C(33)	87.7(4)	89.13(12)
C(31)−Re(1)−C(32)	88.4(4)	88.67(12)
C(32)−Re(1)−C(33)	88.4(4)	89.49(12)
C(31)−Re(1)−N(11)	176.4(3)	173.44(10)
C(32)−Re(1)−N(11)	93.5(3)	95.30(10)
C(33)−Re(1)−N(11)	95.4(3)	96.12(10)
C(31)−Re(1)−N(21)	93.3(3)	91.78(10)
C(32)−Re(1)−N(21)	173.0(3)	173.41(10)
C(33)−Re(1)−N(21)	98.4(3)	97.09(11)
N(11)−Re(1)−N(21)	84.5(2)	83.69(8)
C(31)−Re(1)−Br(1)	93.5(3)	90.37(9)
C(32)−Re(1)−Br(1)	89.9(3)	88.37(9)
C(33)−Re(1)−Br(1)	177.9(3)	177.81(9)
N(11)−Re(1)−Br(1)	83.40(18)	84.54(6)
N(21)−Re(1)−Br(1)	83.23(16)	85.05(6)
N(12)−C(1)−N(22)	109.9(6)	110.6(2)

Figure 6 shows the ORTEP diagrams of the bimetallic molecules of {μ-*m*-[CH(pz)$_2$]$_2$C$_6$H$_4$}[Re(CO)$_3$Br]$_2$·CH_3CN (**3**·CH_3CN) and {μ-*p*-[CH(pz)$_2$]$_2$C$_6$H$_4$}[Re(CO)$_3$Br]$_2$·3C_3H_6O (**4**·3C_3H_6O). Selected bond distances and angles for **3** and **4** are given in Tables 3 and 4, respectively. In both structures the two bis(pyrazolyl)methane sites are on opposite sides of the central phenylene ring. The

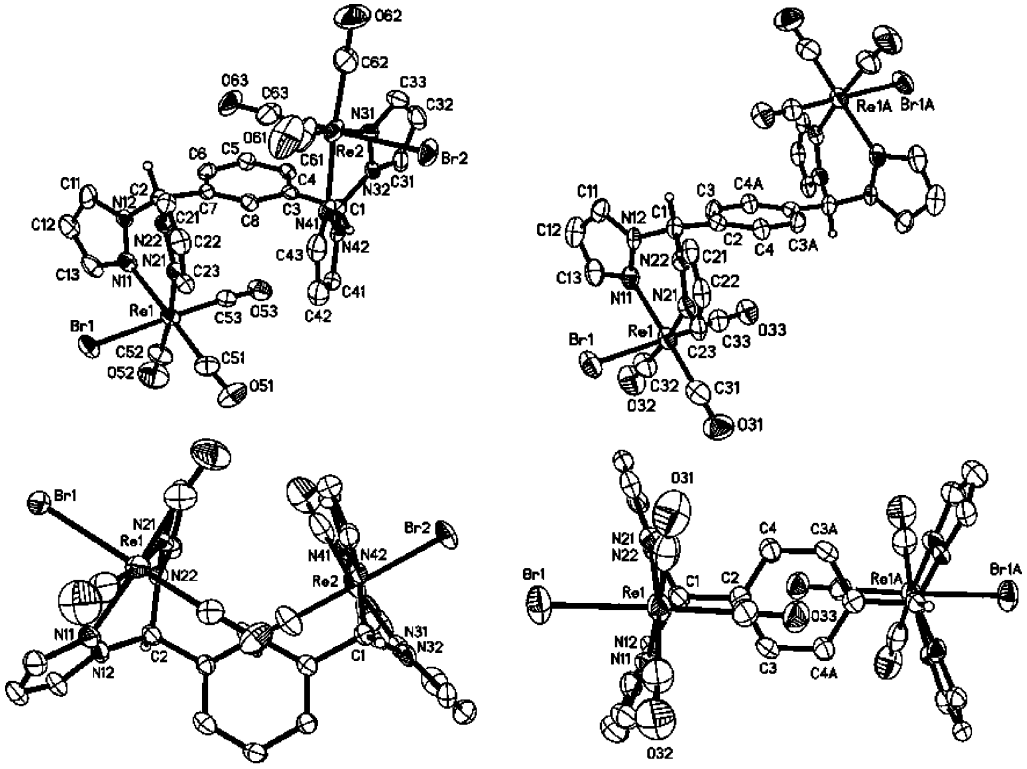

3 **4**

Figure 6. Orthogonal views of the bimetallic molecules of {μ-*m*-[CH(pz)$_2$]$_2$C$_6$H$_4$}[Re(CO)$_3$Br]$_2$·CH_3CN (**3**·CH_3CN) (left) and {μ-*p*-[CH(pz)$_2$]$_2$C$_6$H$_4$}[Re(CO)$_3$Br]$_2$·3C_3H_6O (**4**·3C_3H_6O) (right). Ellipsoids are drawn at the 40% (**3**) and 50% (**4**) probability levels. Hydrogen atoms are omitted.

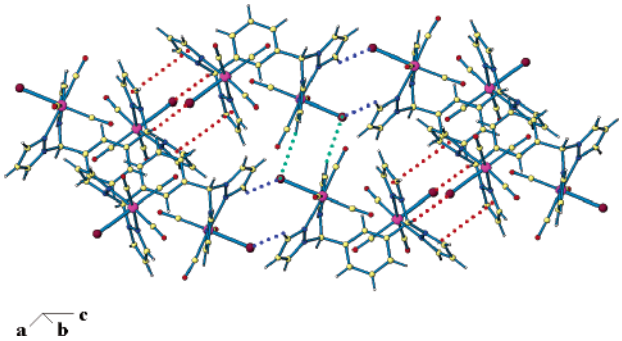

Figure 7. View of **3**·CH_3CN showing distinct CH···Br hydrogen bonds as well as $\pi\cdots\pi$ interactions.

carbonyl groups in the crystal structure of the *para*-derivative are positioned directly over the centroid of the phenylene spacer, whereas the same groups in the *meta*-derivative are offset from the centroid such that edge-centered rather than face-centered interactions exist.

As with the other *meta*-phenylene-linked complexes, intramolecular CH···π interactions between the *ortho* hydrogen atom H(8) and the nearby N(21)- and N(41)-containing pyrazolyl rings in **3** are present and explain the upfield shift of this proton in solution. In addition, the 4- and 6-protons on the phenylene linker (H(4) and H(6)) show CH···π interactions with the nearby N(31)- and N(11)-containing pyrazolyl rings, respectively. The phenylene protons in the *para*-phenylene-linked complex **4** are equivalent in solution and are shielded to an extent comparable to the 4- and 6-protons of the *meta*-phenylene-linked derivatives. This shielding can also be explained by the ca. 2.8 Å CH···π interactions between H(3) and H(4), which are crystallographically nonequivalent, and the nearby pyrazolyl rings containing N(11) and N(21), respectively.

The supramolecular structure of **3**·CH_3CN is dominated by CH···Br hydrogen bonds. The two bis(pyrazolyl)methane units in each molecule are crystallographically nonequivalent, and each unit forms distinct hydrogen bonds. One unit is oriented toward its identical site on an adjacent molecule such that weak $\pi\cdots\pi$ stacking between the appropriate pyrazolyl rings occurs along with reciprocal CH···Br interactions between the Br and methine hydrogen atoms (Figure 7, red dashed lines). A shorter CH···Br interaction exists between the bromine atom of the other bis(pyrazolyl)methane unit and an adjacent 3-pyrazolyl hydrogen atom. This interaction is again reciprocal (Figure 7, blue dashed lines). The combination of these two hydrogen bonds results in the formation of chains. These chains are joined into two-dimensional sheets by the short CH···Br bonds between the latter bromine atoms mentioned above and 3-pyrazolyl hydrogen atoms on adjacent chains (Figure 7, green dashed lines). Finally, the sheets stack upon one another along the *b*-axis by CH···O interactions between CO ligands and a 5-pyrazolyl hydrogen atom on adjacent sheets (not pictured), thus completing the three-dimensional structure.

The extended structure of **4**·$3C_3H_6O$ exhibits a pyrazolyl embrace, as illustrated in Figure 8a, with distances in the upper range of those previously encountered.[7b] The centroid···centroid distance of 3.81 Å is within the usual ranges (red dashed line), but the CH···π bonds

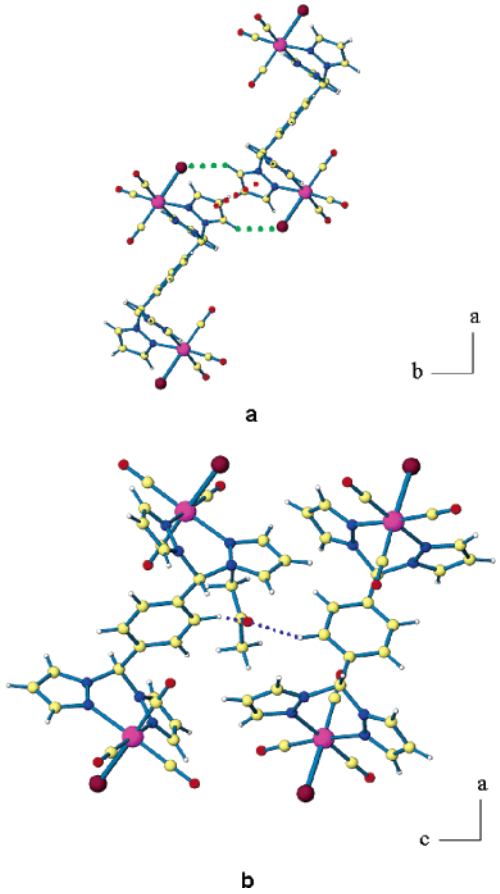

Figure 8. Views of **4**·$3C_3H_6O$ showing (a) the pyrazolyl embrace (only the $\pi\cdots\pi$ stacking of the embrace is indicated, red dashed lines) and supporting CH···Br interactions (green dashed lines) forming chains in the *ab*-plane and (b) two molecules bridged by an acetone (blue dashed lines) leading to chains along the *c*-axis.

are long at 3.44 Å (C(22)H(22)···Ct angle 147°). Supporting the embrace is a CH···Br hydrogen bond involving the 5-pz hydrogen atom H(21) (green dashed lines). There are two distinct chains of molecules formed from the embrace, both in the *ab*-plane.

In contrast to the previous complexes discussed, the three-dimensional supramolecular structure of **4**·$3C_3H_6O$ is organized by solvent−complex interactions. One of the three crystallographic types of acetone molecules in the structure bridges two adjacent molecules through CH···O interactions between the acetone oxygen atom O(42) and the aryl proton H(3) on two symmetry-equivalent phenylene linkers (Figure 8b). This bridging interaction results in chains along the *c*-axis that are orthogonal to the pyrazolyl embrace chains. The chains formed from the pyrazolyl embrace, which exist in the *ab*-plane, alternate direction of propagation. That is, as one pyrazolyl embrace chain runs diagonally from top right to left bottom in the view shown in Figure 9 (red dashed lines), the next chain runs above and below it along the *c*-axis, running from top left to right bottom. The bridging hydrogen bonds involving acetone molecules are shown by the blue dashed lines and connect the pyrazolyl embrace chains along the *c*-axis. The combination of the pyrazolyl embrace and the CH···O hydrogen bonds involving the solvent results in a three-dimensional network that contains columnar voids that

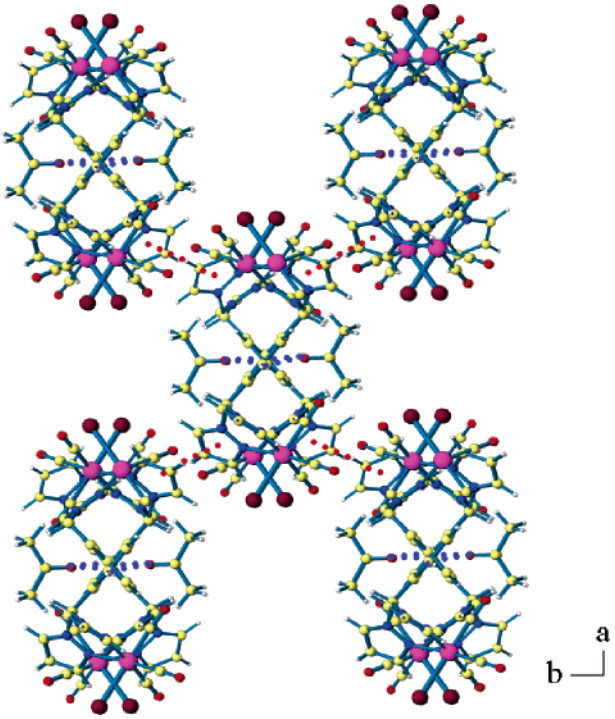

Figure 9. View of **4**·$3C_3H_6O$ down the *c*-axis emphasizing columnar arrangement of the bimetallic molecules formed by the combination of the pyrazolyl embrace (red dashed lines) and bridging acetone molecules (blue dashed lines).

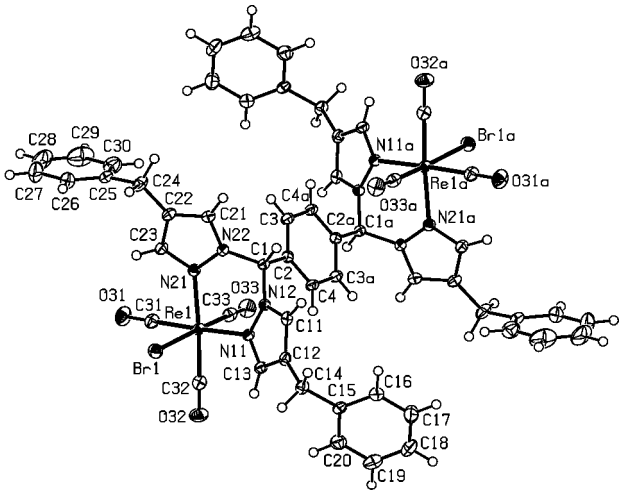

Figure 10. ORTEP drawing showing the bimetallic molecule of {μ-*p*-[CH(^{4Bn}pz)$_2$]$_2$C$_6$H$_4$}[Re(CO)$_3$Br]$_2$·Et$_2$O·4DMSO (**5**·Et$_2$O·4DMSO). Displacement ellipsoids are drawn at the 50% probability level.

extend down the *c*-axis, in the same direction in which the solvent-bridged chains propagate (Figure 9). The columnar voids are filled by the remaining two types of acetone molecules (not pictured). Of these two types, the one containing O(41) is also involved in a CH···O hydrogen bond with the methine proton H(1), but this interaction does not result in extended structure.

An ORTEP diagram of the bimetallic molecule of {μ-*p*-[CH(^{4Bn}pz)$_2$]$_2$C$_6$H$_4$}[Re(CO)$_3$Br]$_2$·Et$_2$O·4DMSO (**5**·Et$_2$O·4DMSO) is shown in Figure 10, and selected distances and angles are given in Table 4. The ether molecule and one of the DMSO molecules of solvation are disordered. As observed in the other bimetallic structures the metal units are oriented on opposite sides of the linking

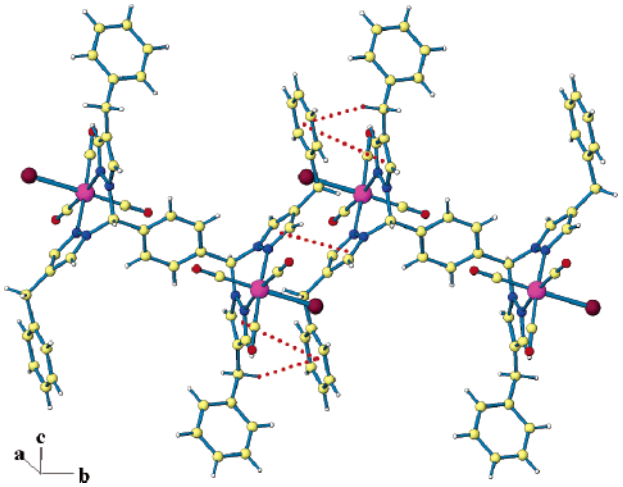

Figure 11. View of bimetallic molecules of **5**·Et$_2$O·4DMSO showing $\pi\cdots\pi$ and CH$\cdots\pi$ interactions. Solvent molecules are excluded.

phenylene ring with a carbonyl ligand from each in a $\pi\cdots\pi$ stacking position. An intramolecular interaction exists between C(4)−H(4) and the pyrazolyl ring containing C(11) (CH···Ct distance = 2.75 Å, CH···Ct angle = 126°) and again explains the upfield shift of the proton resonances in the NMR spectrum. Although H(3) does not show similar bonding in the crystal, C(4) and C(3) are equivalent in solution.

The poor solubility of **5**·Et$_2$O·4DMSO is explained by the extensive $\pi\cdots\pi$ stacking present in the solid state. The structure comprises chains of molecules along the *b*-axis held together by pyrazolyl−pyrazolyl (pz−pz) and phenyl−pyrazolyl (Ph−pz) $\pi\cdots\pi$ stacking between adjacent molecules (Figure 11). The rings involved in pz−pz interactions, which are between adjacent molecules through the respective rings containing C(11), are perfectly parallel, but the stacking is offset significantly (slip angle = 36°) such that the closest interactions are between the C(11)−C(12) edges with an edge to edge distance of 3.56 Å and perpendicular distance of 3.49 Å. There are two Ph−pz interactions for each of the pz···pz interactions. They are related by an inversion center and involve the pz ring containing C(21) and the Ph ring containing C(15). Again the rings are nearly perfectly parallel but offset by 35°. The edge containing C(15) and C(16) is 3.90 Å from the pz ring centroid.

In this structure there are also CH$\cdots\pi$ interactions between the benzyl protons and phenyl groups of adjacent molecules. These interactions re-enforce the $\pi\cdots\pi$ interactions along the *b*-axis (Figure 11). In the crystal the chains of molecules along the *b*-axis are joined together by intercalated DMSO (ordered and disordered) and diethyl ether molecules. The solvent molecules interact with the phenyl rings from the benzyl substituents. The remaining three-dimensional extended structure, therefore, is dominated by solvent interactions.

A remarkable feature of the compounds **1**−**5** presented above is that only one isomer of each respective complex was formed during the syntheses. During characterization of the bulk products, which represented the only isolable metal complex products of the reactions, the lack of proton resonances corresponding to isomeric products in the NMR spectra and the simplicity

Table 5. Distances for C≡O···Ph $\pi\cdots\pi$ Interactions in Rhenium Complexes

compound	centroid C≡O···centroid Ph distance/Å	centroid C≡O···Ph plane perpendicular distance/Å
1	3.16	3.10
2·Et_2O	3.11	3.05
3·CH_3CN	3.37, 3.60	3.08, 3.12
4·$3C_3H_6O$	3.24	3.19
5·Et_2O·4DMSO	3.53	3.20

of the carbonyl absorption regions in the infrared confirmed their isomeric purities. The facial arrangement of the CO ligands about rhenium is consistent with what is expected from the *trans* effect in the $Re(CO)_5Br$ starting material. For this facial arrangement, two isomers may be formed upon coordination by the bis(pyrazolyl)methane donor. The only one observed for any of these complexes is the isomer in which the bromine atom attached to rhenium is oriented *cis* to the methine proton in the boat or twist boat conformation of the six-membered metallacycle. This isomer can orient one of the CO ligands on rhenium in a position to participate in $\pi\cdots\pi$ interactions with the central phenylene ring; the other isomer would place the bromine in this position. Table 5 gives for each complex the distance from the phenylene ring centroid to the center of the proximate C−O bond as well as the perpendicular distance from the phenyl plane to the center of the C−O bond. Since the perpendicular distances of strong $\pi\cdots\pi$ stacking interactions average 3.3−3.6 Å,[22] the complexes presented here exhibit rather strong $\pi\cdots\pi$ interactions between the CO ligands and the linking phenylene ring. The greater the CO ligands are offset from the center of the phenylene ring, as in the structures of **3** and **5**, the greater the difference between the centroid(CO)···centroid(Ph) distance and the centroid(CO)··· plane perpendicular distance.

In previous work with rhenium complexes of bis(pyrazolyl)methane ligands,[23] we proposed that weak intramolecular CH···Br interactions in the transition state of the reacting $[Re(CO)_3Br]$ unit and the ligands directed the formation of a single geometrical isomer analogous to those found in this work. It is reasonable to assume that the same directing force is responsible for the isomeric purity of the current complexes and that additional stabilizing $\pi\cdots\pi$ interactions are also present between the CO ligands and the phenylene linkers, a feature absent from the previous work.

Conclusions

We have demonstrated a direct route to the first heterobimetallic bis(pyrazolyl)methane complex by using the ligand *m*-$C_6H_4[CH(pz)_2]_2$ ($\mathbf{L_m}$), in which the two bidentate donor sites are linked by a rigid phenylene spacer. In this chemistry, the tricarbonylrhenium(I) monometallic complex {*m*-$[CH(pz)_2]_2C_6H_4$}$Re(CO)_3Br$ (**1**) was isolated in low but synthetically useful yield. The use of bidentate poly(pyrazolyl)methane units in our rigid bitopic ligands, especially when oriented in the *meta* position, has led to much more soluble complexes than in our previous work with analogous rigid bitopic tridentate ligands,[9] for which we were unable to isolate a monometallic complex, presumably because solubility problems prevented useful separation procedures.

The monometallic complex **1** was readily converted to the heterobimetallic complex {μ-*m*-$[CH(pz)_2]_2C_6H_4$}-$[Re(CO)_3Br][Pt(p\text{-tolyl})_2]$ (**2**) in good yield, the first such complex that we have been able to prepare with any of our multitopic poly(pyrazolyl)methane ligands**.** We also prepared fixed-geometry homobimetallic rhenium complexes of $\mathbf{L_m}$ ({μ-*m*-$[CH(pz)_2]_2C_6H_4$}$[Re(CO)_3Br]_2$, **3**) and *p*-$C_6H_4[CH(pz)_2]_2$, $\mathbf{L_p}$ ({μ-*p*-$[CH(pz)_2]_2C_6H_4$}$[Re(CO)_3Br]_2$, **4**), as well as of the 4-benzylpyrazolyl derivative *p*-$C_6H_4[CH(^{4Bn}pz)_2]_2$, $^{4Bn}\mathbf{L_p}$ ({μ-*p*-$[CH^{4Bn}(pz)_2]_2C_6H_4$}-$[Re(CO)_3Br]_2$, **5**).

The crystal structures of these complexes formed from fixed-geometry bitopic ligands exhibit significant noncovalent interactions that result in extended supramolecular structures, in much the same way as observed previously with flexible and semirigid ligands.[7,8] The pyrazolyl embrace interaction dominates the structures of **1** and **4**, whereas CH···X (X = O, Br) hydrogen bonds are more important for compounds **2** and **3**. Finally, introduction of the benzyl substituent on the pyrazolyl rings of the ligand in compound **5** leads to strong $\pi\cdots\pi$ interactions dominating the supramolecular structure, demonstrating that we can substantially influence the supramolecular structures by simple substitutions on the pyrazolyl rings. These additional noncovalent interactions manifest themselves in this compound's poor solubility in most common organic solvents.

The rigid phenylene-linked ligands introduced here show promise toward the goal of preparing heterometallic complexes, and additionally, they provide ample comparisons to their more flexible counterparts concerning their supramolecular chemistry.

Acknowledgment. We thank Dr. Radu Semeniuc for helpful discussion, Dr. James Gardinier for a sample of 4-benzylpyrazole, and the National Science Foundation (CHE-0414239) for financial support. We also thank the Alfred P. Sloan Foundation and the EPSCoR program of the state of South Carolina for support of R.P.W. The Bruker CCD single crystal diffractometer was purchased using funds provided by the NSF Instrumentation for Materials Research Program through Grant DMR:9975623.

Supporting Information Available: X-ray crystallographic files in CIF format for all structures reported, including that of *m*-$[CH(pz)_2]_2C_6H_4$. Written and graphical descriptions of the structure of *m*-$[CH(pz)_2]_2C_6H_4$ in text format. This information is available free of charge via the Internet at http://pubs.acs.org.

OM049112F

(22) Janiak, C. *J. Chem. Soc., Dalton Trans.* **2000**, 3885.
(23) Reger, D. L.; Gardinier, J. R.; Pellechia, P. J.; Smith, M. D.; Brown, K. J. *Inorg. Chem.* **2003**, *42*, 7635.